

# Impact of Inverter-based Resources on Impedance-based Protection Functions

Mohammad Zadeh, Prashanth Kumar Mansani  
ETAP

Ilia Voloh  
GE Renewable Energy

Originally presented at the  
46<sup>th</sup> Annual Western Protective Relay Conference, October 2020

# Impact of Inverter-based Resources on Impedance-based Protection Functions

Mohammad Zadeh, Prashanth Kumar Mansani  
ETAP  
Irvine, CA, USA

Iliia Voloh  
GE Renewable Energy  
Markham, Canada

**Abstract**— Inverter-based resources (IBRs) may inject non-conventional or no negative-sequence current during unbalanced faults. The adverse impact of such fault current characteristic has been reported on fault type identification and directional functions that are essential to impedance-based protection. However, the impact of IBR negative current injection on the core part of different implementations of impedance-based protection function has not been thoroughly investigated. Latest German Grid Code introduces a new requirement for IBRs to inject negative sequence current proportional to its measured negative sequence voltage. In this paper, we will investigate if this requirement can address challenges and issues raised by IBRs for protection relays. This paper investigates and compares the impact of IBRs with two options 1- no negative sequence current injection and 2- negative sequence current injection based on latest German code on phase comparator based methods and impedance-based protection functions. Theoretical analysis, software simulation and commercial relay test have been used for this investigation.

**Keywords**— *Inverter; impedance protection, negative-sequence current injection*

## I. INTRODUCTION

The response of inverter-based resources (IBRs) for power system faults heavily depends on its control logic and settings. Most of the conventional inverters only inject positive-sequence current while some inverters inject negative-sequence current to reduce the size of capacitor at the DC side of the inverter. This negative-sequence current does not match with the negative-sequence fault current characteristic of a synchronous machine. As a result, it may result in false trip of protective relays that are designed and operated based on fault current characteristics of synchronous machines.

There has been increase in awareness in the power system community about the importance of injecting negative sequence current by IBRs during fault with right characteristics. German Grid Code updated in 2017 mandated IBRs to be capable of injecting negative sequence current proportional to its measured negative sequence voltage [1] during the fault. Latest draft of IEEE P2800 [2] also enforces IBRs to inject negative sequence similar to latest German Grid Code. More details of the characteristic of negative sequence current injection required by this code are provided in the paper. Although the magnitude of IBR fault current is considerably limited as compared to a synchronous machine because of lower short-circuit limit, the phase angle of positive and negative sequence currents with

respect to IBR terminal positive and negative sequence voltages will be similar to a synchronous machine as per latest German code.

Typical impedance-based protection functions depend on 1-phase selection, 2- fault direction and 3- fault-loop impedance comparison with its corresponding characteristics. The adverse impact of lack or improper IBR negative sequence current injection on phase selection and directional functions have been discussed in other papers as reported in [3]. Authors assume that these issues can be mitigated either by using different techniques or by new Grid codes that mandate negative-sequence current injection similar to synchronous generators. The impact of IBR on distance functions was studied by authors in [4], [5]. In this work, both phase-to-ground and phase-to-phase loop is analyzed. In addition, an updated wind farm model is used for more realistic results.

Relay vendors have utilized different methods to implement impedance-based protection functions. Some vendors use phase comparators while others estimate the impedance of faulted-loop to compare against characteristics. The combination of both techniques has been employed as well. In this work, the implementation of different types of impedance-based protection functions is presented and for each type, the seen impedance equation is shown for performance comparison. Phase comparator-based techniques are also covered as part of the discussion for phase-to-ground, phase-to-phase and phase-to-phase-to-ground faults. Theoretical and simulation analyses are provided to determine how each method is affected by the lack of negative sequence current from IBR. The performance of each calculation method is compared against the case where the IBR injects negative sequence current as per recent German code [1].

## II. DISTANCE PROTECTION

Impedance/Distance protection function is widely used in transmission and sub-transmission protection applications due to high speed, selectivity and reliable operation. In distance protection, estimated impedance between relay and fault location is compared directly or indirectly against a characteristic using voltage and current measurements at the relay location. Multiple approaches have been utilized by the relay vendors to implement distance protection function. Today's state-of-the-art distance relays employ microprocessor-based technology due to increased accuracy, less maintenance,

ability to facilitate multiple functions. Within microprocessor-based relay technology, from the implementation point of view, it is possible to classify the impedance-based protection function into 1- phase-comparator-based and 2- impedance-measurement-based methods. Each method and its variation are discussed briefly in the following. However, the impact of IBR fault current characteristic particularly lack of negative sequence current is highlighted.

#### A. Phase-comparator-based Method

Phase-comparators compare the phase angle difference between two phasors called polarizing and operating signals. The comparator output is set to true otherwise false if the angle of operating signal compared to the polarizing signal falls within a specified range. Different types of characteristics such as mho, reactance representing the boundary of operation can be created by selecting multiplying coefficients. In the following, basic implementation of Mho and Quadrilateral ground functions based on the phase comparator technique are presented.

1) *Mho characteristic*: The basic mho characteristic for AG fault is formed by the polarizing and operating signals as shown below.

$$S_{Pol} = V_{mem1(A)} \quad (1)$$

$$S_{Opr} = -V_a + Z_{Set}(I_a + K_0 I_0) \quad (2)$$

where,  $V_{mem1(A)}$  is the positive-sequence memory voltage for AG loop,  $Z_{Set}$  is the user reach setting with line angle,  $K_0$  is the zero-sequence compensation factor given by  $Z_0/Z_1-1$ ,  $I_0$  is the zero-sequence current and  $V_a$  and  $I_a$  are the phase A voltage and current [6]. For the seen impedance to fall within the mho characteristic, the difference between polarizing and operating signal should fall between  $-90^\circ$  and  $90^\circ$ . Similar comparators exist for phase BG and phase CG fault loops.

Phase comparators are widely used for phase-phase fault protection. For BC fault loop, the polarizing and operating signals are given by (3) and (4).

$$S_{Pol} = V_{mem1(bc)} = j V_{mem1} \quad (3)$$

$$S_{Opr} = -V_{bc} + Z_{Set} I_{bc} \quad (4)$$

where  $V_{mem1(bc)}$  is the line positive-sequence memory voltage for BC loop, and  $V_{bc}$  and  $I_{bc}$  are line voltage and current for BC loop [3]. Memory voltage is used to mitigate lack of voltage during closing fault where the measured voltage is close to zero and its angle estimation is not available. The philosophy behind using memory voltage is that the angle of the polarizing signal, pre-fault and during a fault remains relatively constant for a typical power system application. This is valid for strong sources, however for weak sources, the phase angle of relay measured voltage changes considerably. This angle change results in dynamic expansion [3] of mho characteristic that increases resistive coverage of the relay. This is advantageous because higher fault resistance is expected for weak sources.

The polarizing and operating signals for the mho characteristics are formed using phase current and voltage. Hence, mho relay is not directly affected by the lack of negative-sequence current from the IBRs. However, as will be shown later

through software simulation, the mho characteristic expands less in case of IBR with just positive sequence injection as compared to an IBR with both positive and negative sequence injection based on latest German code.

2) *Quadrilateral characteristic*: Quadrilateral characteristic are usually employed for detecting phase-to-ground faults. A simple characteristic can be implemented using four comparators as shown in Table 1. Here,  $Z_{Rev}$  is the reverse reach settings,  $Z_R$  is right blinder characteristic impedance and  $Z_L$  is the left blinder characteristic impedance. Reverse reactance comparator can be replaced with a phase comparator to create directional quadrilateral ground function. For reactance comparator, phase current, superimposed phase current, zero-sequence current, or negative sequence current can be used as a polarizing signal.

Modern protective relays widely use negative sequence as conventional negative-sequence networks are more homogenous [7]. Non-conventional or no negative sequence current injection of IBRs results in mal-operation of quadrilateral element based on negative sequence polarization. In addition, directional phase comparator may use negative-sequence current as a polarizing signal that in this case is also susceptible to mal-operation.

Table 1 Quadrilateral characteristics comparators

Characteristic	Polarizing signal	Operating signal
Reactance	$jI_0$ or $jI_2$	$Z(I + K_0 I_0) - V$
Reverse reactance	$jI_0$ or $jI_2$	$Z_{Rev}(I + K_0 I_0) - V$
Right blinder	$Z_R(I_a + K_0 I_0)$	$-V + Z_R(I_a + K_0 I_0)$
Left blinder	$Z_L(I_a + K_0 I_0)$	$-V + Z_L(I_a + K_0 I_0)$

#### B. Impedance-Measurement (IM)-based Methods

In IM-based approach, estimated impedance or a combination of estimated resistance and reactance are compared against a specified characteristic or thresholds defined by user settings. These methods are typically used to implement quadrilateral or directional impedance characteristics.

For a fault at distance  $m$  from the relay, the voltages seen by the relay for A-to-ground fault and BC fault are given by,

$$V_a = mZ_1 I_1 + mZ_2 I_2 + mZ_0 I_0 + R_F I_F \quad (5)$$

$$V_{bc} = mZ_1 I_{bc} + R_F I_F \quad (6)$$

where,  $Z_0$ ,  $Z_1$ , and  $Z_2$  are the sequence impedances of the line,  $I_0$ ,  $I_1$ , and  $I_2$  are the sequence currents,  $I_F$  is the fault current, and  $R_F$  is the fault resistance. Simplifying (5) yields,

$$V_a = mZ_1 (I_a + K_0 I_0) + R_F I_F \quad (7)$$

Apparent impedance estimation methods employed by relay vendors can be broadly classified into four types as summarized below. These four methods are usually employed for phase-to-ground fault loops, however method III is employed by at least one major relay vendor for phase-to-phase fault loops.

1) *Method I*: In this method,  $mZ_1$ , positive-sequence impedance for phase-to-ground fault loop, is estimated by

assuming  $R_F$  as zero in (5). Therefore, the estimated impedance  $mZ_1$  is given by:

$$mZ_1 = V_a / (I_a + K_0 I_0) \quad (8)$$

Here, fault resistance is neglected in the impedance calculation, as a result an error is introduced in the estimated impedance as shown below:

$$\text{Error} = (R_F I_F) / (I_a + K_0 I_0) \quad (9)$$

The error is introduced in both estimated resistance and reactance. Typical values for  $K_0$  are greater than 1, therefore estimated fault resistance is considerably smaller than the original value. The error is generally approximated as  $R_F/(1+K_0/3)$  and it is usually compensated by multiplying the desired resistive coverage with the correction factor.

2) *Method II*: Equation (5) can be written as,

$$V_a = mR_1 I_R + jmX_1 I_X + R_F I_F \quad (10)$$

where  $I_R = I_a + (R_0/R_1 - 1) I_0$  and  $I_X = I_a + (X_0/X_1 - 1) I_0$  in the above equation. Assuming  $\angle I_F \approx \angle I_R$  and solving (10) yields,

$$mX_1 = \frac{\text{Im}\{V_a\} \text{Re}\{I_R\} - \text{Re}\{V_a\} \text{Im}\{I_R\}}{\text{Re}\{I_X\} \text{Re}\{I_R\} + \text{Im}\{I_X\} \text{Im}\{I_R\}} \quad (11)$$

$$R_{\text{seen}} = \frac{\text{Im}\{V_a\} \text{Im}\{I_X\} + \text{Re}\{V_a\} \text{Re}\{I_X\}}{\text{Re}\{I_X\} \text{Re}\{I_R\} + \text{Im}\{I_X\} \text{Im}\{I_R\}} \quad (12)$$

Assuming  $I_F = I_a$ , i.e., no feed from the remote end, the approximate error in the estimated resistance can be calculated by

$$R_{\text{seen Error}} = R_F / (1 + K_r) \quad (13)$$

where,  $K_r$  is  $(R_0/R_1 - 1)/3$ . The estimated fault resistance estimated by this method is smaller as compared to the actual value similar to Method I, and the desired resistive coverage is achieved by using a correction factor. In Method II, the approximate error in the estimated reactance becomes zero that is advantageous as compared to Method I [8]. Also, phase current is used for impedance estimation so this method is affected by the infeed.

3) *Method III*: This method is based on a conventional single-ended fault location algorithm for transmission line application [9]. This method can be employed for phase-to-ground fault and phase-phase fault.

*Phase-to-ground loop*:

In this approach, estimated resistance and reactance are given by,

$$mX_1 = \text{Im}\{V_a \times I_F^*\} / \text{Im}\{(R_1/X_1 + j)(I_a + K_0 I_0) I_F^*\} \quad (14)$$

$$R_F = \text{Im}\{V_a (Z_1^* (I + K_0 I_0))^*\} / \text{Im}\{I_F (Z_1^* (I + K_0 I_0))^*\} \quad (15)$$

$$R_{\text{seen}} = mR_1 + R_F = (mX_1) \times (R_1/X_1) + R_F \quad (16)$$

where,  $R_F$  is the estimated fault resistance. Relay vendors [10][11] may use 1)  $3I_0$ , 2)  $1.5 \times I_0 + 1.5 \times I_2$ , and 3)  $3I_2$  to estimate  $I_F$  in (14) and (15). For an IBR with non-conventional or no negative sequence current injection, the choice of  $I_F = 3 \times I_2$  will not be acceptable. From (14), it can be inferred that the estimated reactance is independent from estimated fault current magnitude. Therefore, the choice of  $1.5 \times I_0 + 1.5 \times I_2$  as an estimate of  $I_F$  has no significant impact on the estimated reactance as far as negative-sequence current injected by IBR is zero or small. However, an error is introduced in the estimated resistance as the term  $I_F$  is only in the denominator.

*Phase-to-phase loop*:

Equating real and imaginary parts of (6) and solving yields the following equations,

$$mX_1 = \text{Im}\{V_{bc} \times I_{\text{comp}}^*\} \sin\phi / \text{Im}\{(R_1/X_1 + j)I_{bc} I_{\text{comp}}^*\} \quad (17)$$

$$0.5R_F = \text{Im}\{V_{bc} (Z_1 I_{bc})^*\} / \text{Im}\{2 I_{\text{comp}} (Z_1 I_{bc})^*\} \quad (18)$$

where,  $I_{\text{comp}}$  is the compensating current and  $\phi$  is the angle of line impedance [12]. The total seen resistance by the relay is calculated by using (16) and it is used for LL as well as LLG faults. Since zero-sequence current is only available for LLG faults, negative sequence current is used to calculate the compensating current, where  $I_{\text{comp}} = j\sqrt{3} I_2$ . Obviously for an IBR with only positive sequence current injection, this method gives an inaccurate result.

4) *Method IV*: This method is a combination of phase comparator and Method III that is used by at least one of the relay vendors [13]. Here, the seen resistance is estimated using Method III as shown in (16) and a phase comparator is used for seen reactance. If negative sequence is not used as polarizing signal in phase comparator, no considerable impact is expected on the reactance reach. The impact on the resistive reach can be inferred by observing the results from Method III.

### III. FRT REQUIREMENTS

Bulk Power System experiences frequency and voltage disturbances during faults. Previously, IBRs are disconnected from the system if sudden disturbances are seen in frequency or voltage in the transmission system. However, with the increasing penetration of renewable resources, immediate tripping of IBRs could raise reliability concerns. Therefore, FERC mandated fault-ride through (FRT) requirements for IBRs to support the grid during sudden voltage or frequency disturbances [14].

#### A. Dynamic Positive Sequence Support (DPS)

Most of the present-day inverters support positive sequence current injection during system disturbances. The main objective is to support the positive sequence voltage of the system by increasing the positive sequence current injection during fault. The operation of the inverter depends on the IBR control mode. Generic IBR control modes could be classified into three types 1- real power priority 2- reactive power priority 3- power factor control [2]. Depending upon the control mode, active power or

reactive power generation is given priority if the current injection exceeds the inverter current limit. In reactive power priority, IBR may actively curtail the real power to prioritize reactive power injection while in real power priority, IBR may curtail reactive power. In dynamic positive sequence support, IBRs are in reactive power priority mode and inject positive sequence reactive current as shown below,

$$I_{q1} = -jK_1 \times \Delta V_1 = -jK_1 \times |V_{1\text{fault}} - V_{1\text{pre-fault}}| \quad (19)$$

where  $K_1$  is usually chosen between 2 and 7 and  $\Delta V_1$  is typically a negative number. It is important to note here that for close-in faults, the drop in voltage is significant, as a result IBR reaches its maximum current limit being smaller effective  $K_1$  factor. IBRs are set to reactive power priority in this study to analyze the impact of DPS on distance protection functions.

#### B. Dynamic Positive and Negative Sequence Support (DPNS)

During unbalanced faults, the voltage of the system becomes unbalanced and negative and zero sequence components are introduced into the system. Injecting only positive sequence current results into reactive power injection to all phases including healthy phases. This leads to adverse effects on voltage profile and protection functions as discussed in the later section. Therefore, similar to synchronous generators, it is preferred to inject both positive and negative sequence currents. Recent German code as shown in Fig. 1 mandates dynamic grid support of positive and negative sequence current for IBRs during unbalanced faults. Positive and negative sequence currents to be injected into the system are calculated based on the FRT curve as shown in (19) and (20). As discussed earlier, the operation of the IBR depends on its control logic and settings. In this study, equal priority is given to the reactive positive sequence injection and negative sequence injection for any disturbances in the system. IBR tries to maximize the positive sequence voltage and minimize the negative-sequence voltage adhering to the short circuit capacity of the converter.

$$I_{q2} = jK_2 \times \Delta V_2 = jK_2 \times |V_{2\text{fault}} - V_{2\text{pre-fault}}| \quad (20)$$

where  $K_2$  is usually chosen between 2 and 7 and  $\Delta V_2$  is typically a positive number. This approach makes IBR to behave like a synchronous generator with  $1/K_2$  negative-sequence reactance within its current limits.

#### IV. TEST SYSTEM PARAMETERS

A Type-IV wind farm test system of 100 MW capacity is simulated by aggregating 50 wind generators with 2 MW capacity each. Wind generators are connected to the grid through a Yg-D unit transformer and Yg-Yg-D plant transformer and 93.2 mile long transmission line as shown in Fig. 2. The modeled IBR is connected to a grid modeled as voltage source behind a constant impedance with SIR of 0.17. If the current pace in the deployment of renewable energy resources continues in future, most of the renewable stations will be connected to a weak grid. To simulate this scenario, an alternate system is created where the IBR is connected to a weak grid with SIR of 6.23. The  $K$  factor of the IBR is set to 4. As a result, the fault response of the IBR will be similar to a conventional generator with sub-transient reactance of 25%. To study the response of DPS and DPNS for an unbalanced fault, LG, LL and LLG faults are

inserted on interconnected transmission line at various fault locations.

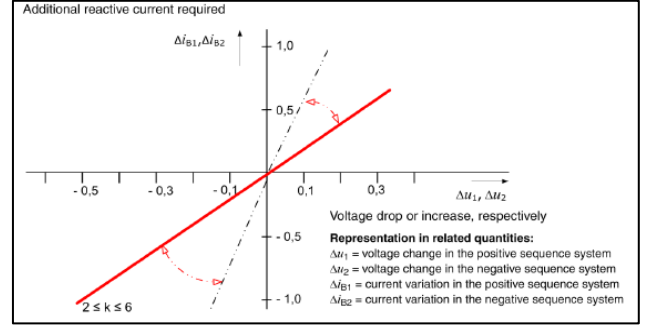


Fig. 1 Germany FRT requirements [1]

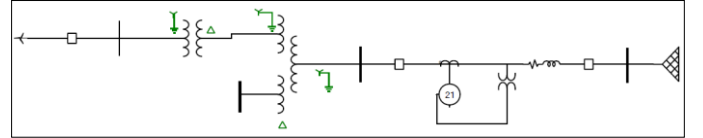


Fig. 2 One-line diagram

#### V. THE IMPACT OF IBR ON POWER SYSTEM CHARACTERISTICS

The behavior of IBRs is fundamentally different from a conventional generator. Lack of or non-conventional negative sequence current injection affects the system voltage magnitude, angle and homogeneity during faults. Therefore, the impact of DPS and DPNS on the system voltage and current profile pertain to protection system is studied using the test system in the following section.

##### A. Voltage profile of unfaulted phases

During unbalanced fault, IBR with DPS detects the drop in the positive sequence voltage of the system. IBR responds to the disturbance by increasing the positive sequence current injection based on FRT requirements to support positive sequence voltage. This supports the faulted phase and increases the voltage as intended. However, since IBR only injects positive sequence voltage, the voltage of the un-faulted phases may increase leading to overvoltage issue. It can be observed in Fig. 3 that during AG fault, the voltage of phase B, C are raised above 100 % with DPS. On the other hand, IBRs with DPNS inject both positive sequence and negative sequence currents during unbalanced faults. As a result, the behavior of the IBR is similar to conventional generators and un-faulted phases do not experience overvoltage.

##### B. Change in voltage angle

During close-in faults, voltage drops to about zero leading to mal-operation of self-polarized mho distance function. Therefore, memory polarization is commonly used in microprocessor-based relays to form a polarizing signal. Use of memory voltage polarization results in dynamic expansion of mho characteristic during fault. The degree of dynamic expansion of mho characteristics depends on the system strength. In a strong system, the change in the voltage angle between fault and pre-fault conditions ( $\angle V_a - \angle V_{1\text{pre-fault}}$ ) will be smaller resulting in a smaller expansion. However, in a weak

system, the change in voltage angle will be larger leading to a larger expansion of mho characteristic.

IBRs with DPS use full converter capacity to support the positive sequence voltage. Therefore, the change in the voltage angle is small as shown in Fig. 4 resulting in smaller expansion. On the other hand, in IBRs with DPNS, the converter capacity is distributed between maintaining positive sequence voltage and negative sequence voltage by injecting current into the faulted phase(s). Therefore, the angle shift of faulted phase angle is higher as compared to the case of positive sequence support (DPS) as shown in Fig. 5, resulting in larger expansion. This is more prominent in a case where IBR is connected to a weak system.

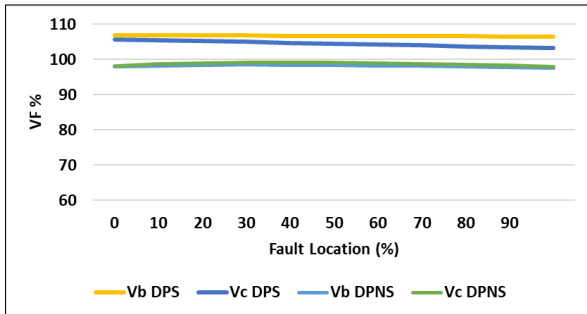


Fig. 3 Voltage of healthy phases during dynamic grid support

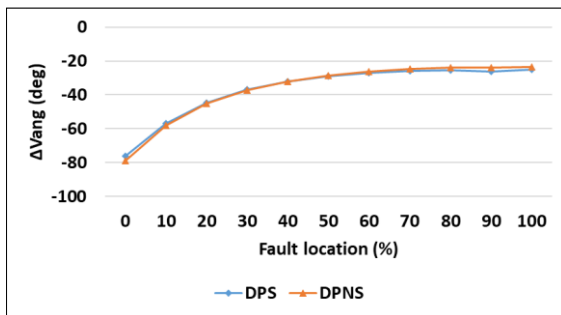


Fig. 4 Voltage angle difference (fault – pre-fault), IBR connected to a strong system

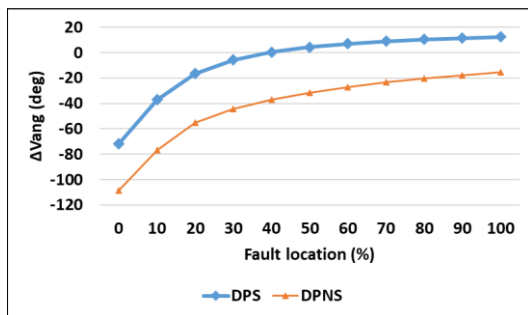


Fig. 5 Voltage angle difference (fault – pre-fault), IBR connected to a weak system

### C. Effect on homogeneity

Impedance-based protection functions need to be properly set to address nonhomogeneous systems. The non-homogeneity creates an angle difference between the current measured by the relay and fault current. The angle difference may adversely impact relay performance if relay is not properly set.

Conventional generators act as a voltage source behind an impedance, therefore the angle difference between the measured source impedance at either end of the line is fixed and is usually compensated using a correction factor. However, IBRs acts as a constant current source with varying impedance. As the source impedance varies with the inverter response, the non-homogeneity varies with fault location for both DPS and DPNS as shown in Fig. 6, where  $\Delta I_{Ang}$  is the angle difference of the faulted phase current ( $\angle I_{IBR(A)} - \angle I_{Grid(A)}$ ). Therefore, non-homogeneity introduced by the IBRs with DPS as well as DPNS affects the impedance-based protection function.

Therefore, it can be concluded that lack of negative-sequence injection results in 1- over-voltage in unfaulted phases, 2- smaller dynamic expansion of memory-polarized Mho characteristic, and unknown non-homogeneity is seen in currents from both sides feeding a fault with and without negative-sequence current injection.

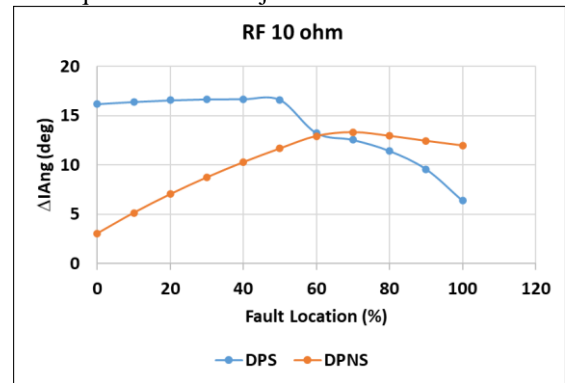


Fig. 6 Effect of DPS and DPNS on the angle difference of the faulted phase

## VI. SIMULATION AND TESTING RESULTS

In this section, the impact of DPS and DPNS on different distance protection methods is discussed in detail for both phase-to-ground and phase-to-phase fault loops.

### A. Phase-to-ground loop

In this section, the impact of IBRs on phase-comparator based methods and IM-based methods for phase-to-ground fault is discussed.

#### 1) Phase-comparator-based method

A phase comparator is modeled with positive sequence memory polarization. As explained in the earlier section, the dynamic expansion of mho characteristics depends on the system strength. IBR with DPS can utilize full converter capacity at disposal to support positive sequence voltage as discussed earlier. Therefore, the dynamic expansion of mho characteristics is expected to be smaller in positive sequence support as compared to the combined positive and negative sequence support. In a strong system, the change in the voltage angle is small. As a result, the resistive coverage of positive sequence support and positive and negative sequence support is almost similar as shown in Fig. 7.

For an IBR connected to a weak system, the change in the voltage angle as compared to the memory voltage is considerable as shown in Fig. 5. As predicted in Section V.B and

shown in Fig. 8, the resistive coverage in DPS is smaller as compared to the IBR with DPNS. In other words, the Mho characteristic expands less when IBR only injects positive sequence as compared to a case where both positive and negative sequence is injected.

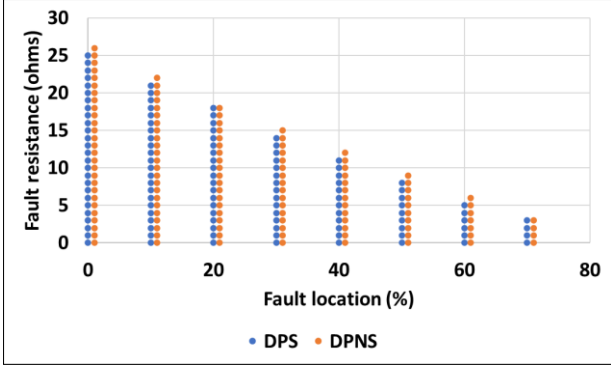


Fig. 7 Expected trip for LG fault in a strong system

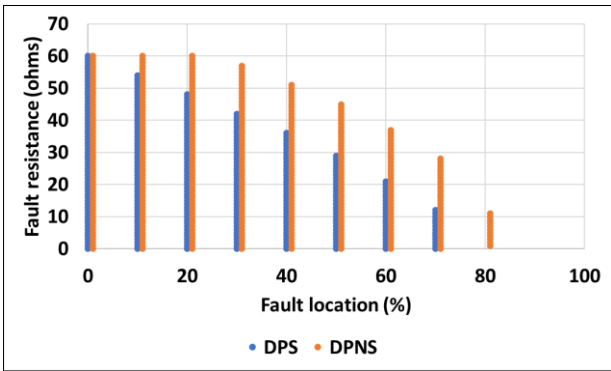


Fig. 8 Expected trip for LG fault in a weak system

In order to further verify the results of simulation, COMTRADE files were generated for phase-to-ground fault for the case of 60 % fault location and played back as an input to GE D60 distance relay [15]. The fault resistance is chosen as 15, and 25 ohms for DPS and 35 and 45 ohms for DPNS to generate COMTRADE files. From Table 2, it can be inferred that the resistive reach in DPS is around 15-25 ohms, whereas in DPNS it is around 35-45 ohms. Therefore, it can be concluded that the resistive reach of the relay in DPS is smaller as compared to the IBR with DPNS. It is important to note that the hardware test results match the simulation results.

Table 2. Actual relay output to play-in COMTRADE cases

IBR injection	Fault location (from IBR)	RF	Expected Trip (ETAP)	Relay output
DPNS	60	35	Yes	Yes
DPNS	60	45	No	No
DPS	60	15	Yes	Yes
DPS	60	25	No	No

## 2) Impedance-Measurement-based (IM-based) Methods

The estimated impedances for Methods I to III are compared with the actual fault impedance to study the impact of IBR as shown below,

$$\Delta R_{\text{seen}} = R_{\text{seen}} - R_F \quad (21)$$

$$\Delta X_{\text{seen}} = X_{\text{seen}} - X_F \quad (22)$$

where,  $R_{\text{seen}}$  and  $X_{\text{seen}}$  correspond to the impedance seen by the line relay at the IBR side and  $R_F$ ,  $X_F$  represent the actual fault resistance and loop reactance, respectively. For line-to-ground fault as mentioned in Section II, Method IV is a combination of Method III and phase comparators, thereby the results can be inferred from each one.

Fig. 9 shows the error in seen resistance of all studied methods for a case of IBR connected to a strong system. As it is shown, Method I is not considerably affected. For Method II and Method III where  $3 \times I_0$  is selected as  $I_F$ , seen resistances are not affected as expected by the presence or lack of negative sequence current. As predicted in Section II.B.3), the error in the estimated resistance is considerable for Method III with  $(1.5 \times I_0 + 1.5 \times I_2)$  as  $I_F$ . Lack of negative sequence current (DPS) results in higher seen resistance error as compared to the case IBR injects both positive and negative sequence currents (DPNS).

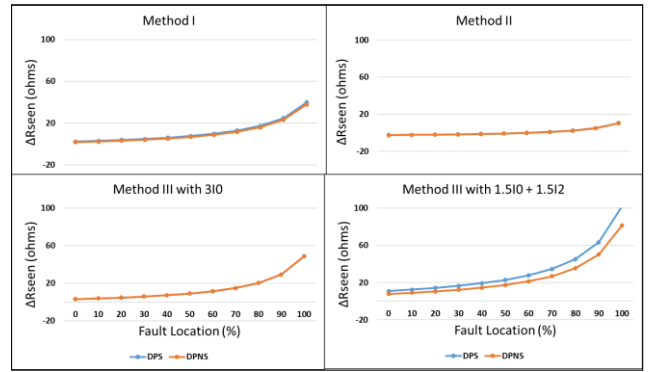


Fig. 9  $\Delta R_{\text{seen}}$  for LG fault in a strong system at  $R_f = 5$  ohms

Fig. 10 shows the error in seen resistance of all studied methods for a case of IBR connected to a weak system. As expected, due to a smaller feed from the grid side, the overall seen resistance error is considerably smaller as compared to a strong system. In addition, as expected, Method II and Method III with  $3I_0$  choice are not impacted by the choice of negative sequence current injection.

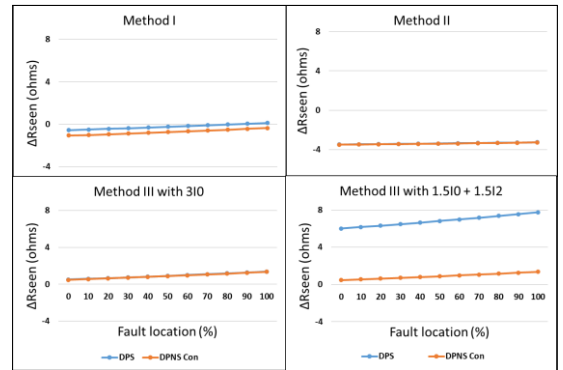


Fig. 10  $\Delta R_{\text{seen}}$  for LG fault in a weak system at  $R_f = 5$  ohms

The impact of negative sequence current injection on the estimated reactance for strong and weak systems is shown in Fig. 11 and Fig. 12, respectively. As it is shown, the choice of negative sequence current injection does not have any

considerable adverse impact on the seen reactance estimation specially for the case where IBR is connected to a strong system.

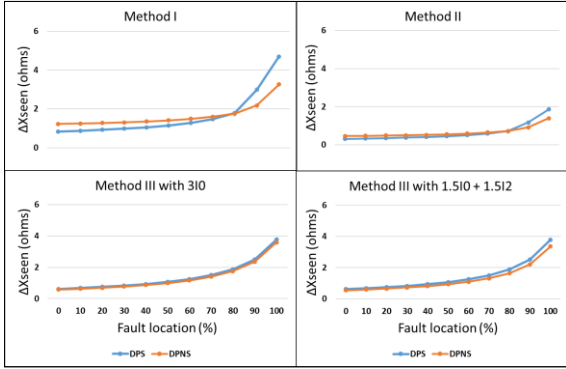


Fig. 11  $\Delta X_{seen}$  for LG fault in a strong system at  $R_f = 5$  ohms

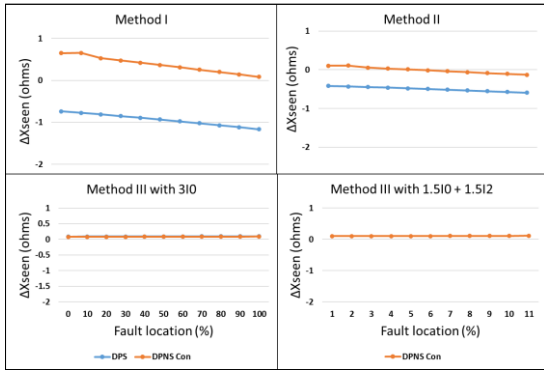


Fig. 12  $X_{seen}$  for LG fault in a weak system at  $R_f = 5$  ohms

### B. Phase-to-phase loop

The impact of IBRs on phase-to-phase fault loop for phase comparator-based and Method III is discussed in the following section.

#### 1) Phase-comparator-based method

For LL faults, as shown in Fig. 13 and Fig. 14, the dynamic expansion of mho characteristic results in increased resistive coverage similar to LG faults. In weak systems, the change in voltage angle results in increased resistive coverage. However, in strong systems, the change in the voltage angle is small. Therefore, the increase in resistive reach is relatively smaller.

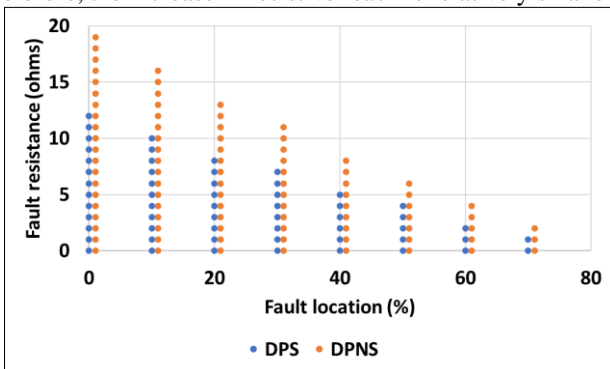


Fig. 13 Expected trip for LL fault in a strong system

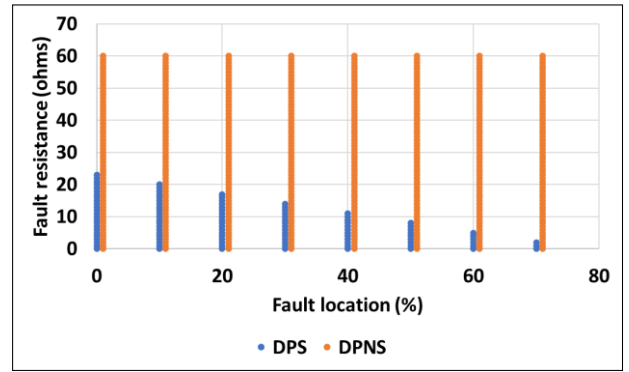


Fig. 14 Expected trip for LL fault in a weak system

For a LLG fault, the fault resistance simulated is between the ground and the joint of faulted phases at the point of fault location. This means that the phase-to-phase fault loop is not affected by the fault resistance. As a result, large resistive coverage is expected and seen for LLG faults (Fig. 15 and Fig. 16) and the reach of the relay is as set irrespective of the fault resistance.

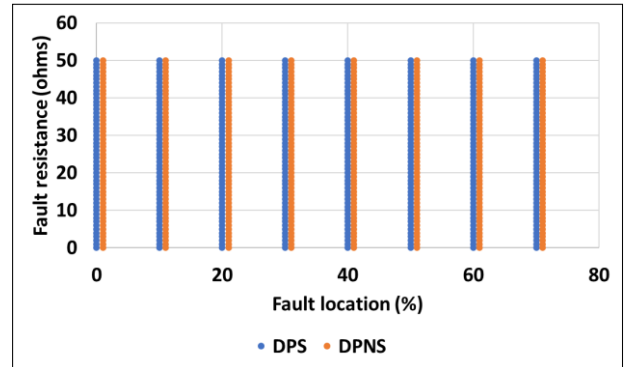


Fig. 15 Expected trip for LLG fault in a strong system

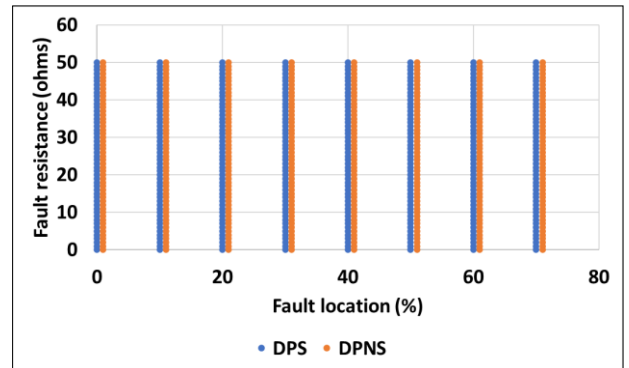


Fig. 16 Expected trip for LLG fault in weak system

#### 2) Impedance-Measurement-based (IM-based) Methods

As discussed in Section II, this method directly employs negative sequence current for impedance estimation, as a result

gives incorrect results for DPS. Use of this method for the protection of interconnection of IBR to grid should be avoided. Since there is no point of showing these results, there is no comparison can be done as well with the performance of Method III for the case of IBR injecting both positive and negative sequence currents, i.e., DPNS. However, expected trip results for DPNS are provided in Fig. 17 - Fig. 20 with resistive reach setting as 20 ohms. For LL fault, as it is illustrated in Fig. 17 and Fig. 18, the resistive reach is reduced by infeed from the grid end. In strong systems, resistive coverage is adversely impacted by the infeed. However, in weak systems, the impact on relay performance is smaller. For LLG fault, relay trips as set regardless of the fault resistance in both strong and weak systems.

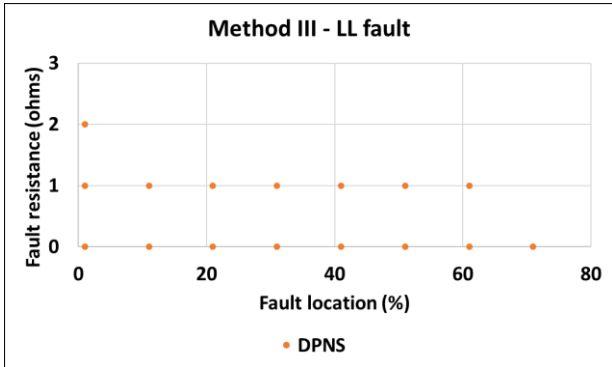


Fig. 17 Expected trip for LL fault in a strong system

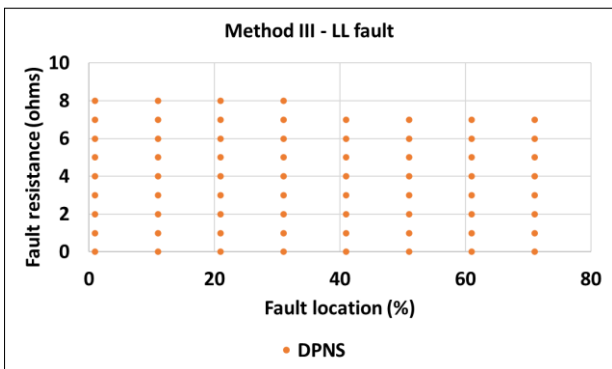


Fig. 18 Expected trip for LL fault in weak system

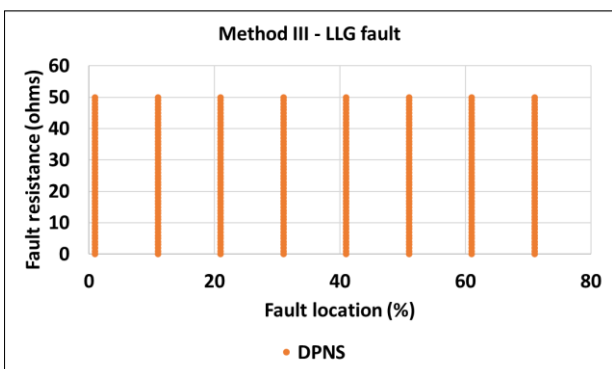


Fig. 19 Expected trip for LLG fault in a strong system

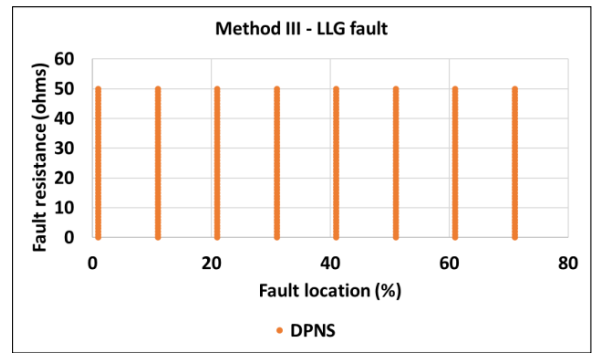


Fig. 20 Expected trip for LLG fault in weak system

## VII. CONCLUSION

Inverter-based resources (IBRs) may inject non-conventional or no negative-sequence current during unbalanced faults. Common commercial techniques used to implement impedance-based protection functions were discussed in this paper. The effect of IBRs with and without negative-sequence injection on impedance-based protection function was investigated. The results for a phase-to-ground faults were validated by testing a commercial relay with software generated COMTRADE files.

Lack of injecting negative sequence current by IBR is found to cause 1) over-voltage in unfaulted phases and 2) smaller dynamic expansion of Mho characteristic. Table 3. summarizes the outcome of this investigates to indicate which methods shall be avoided, which ones are not affected and which ones are affected and in what extent. Both cases of IBRs with no positive sequence current injection (DPS) with respect to the case where both positive and negative sequence current (DPNS) is injected are reported.

Table 3. Summary of results of DPS vs DPNS

Method	LG	LL	LLG
Phase comparator (Mho)	Smaller resistive coverage	Smaller resistive coverage	Not affected
Method I	Not affected	NA	NA
Method II	Not affected	NA	NA
Method III with $3I_0$	Accurate though zero-sequence coupling is not studied	NA	NA
Method III with $3I_2$	Shall be avoided	Shall be avoided	Shall be avoided
Method III with $1.5I_0+1.5I_2$	Adversely impacted	NA	NA

## REFERENCES

- [1] "Summary of the draft VDE-AR-N 4120," May 2017.
- [2] A. Rajapakse, R. Majumder, S. G. R. Energy and R. Nelson, "Modification of commercial fault calculation programs for wind turbine generators," 2020. [Online]. Available: [https://www.pes-psrc.org/kb/published/reports/C24\\_WG\\_Report\\_Jun\\_2020\\_Final.pdf](https://www.pes-psrc.org/kb/published/reports/C24_WG_Report_Jun_2020_Final.pdf)
- [3] "Impact of inverter-based resources on protection schemes based on negative sequence components," EPRI, 2019.
- [4] M.R.D Zadeh, M. P. Kumar, and D. Ting, "Impact of inverter-based resources on impedance-based protection functions," in Proc. Developments in Power System Protection, Liverpool, UK, Mar 9-12, 2020.

- [5] M. Zadeh, M. P. Kumar, and I. Voloh, "Impact of inverter-based resources on impedance-based protection functions," in Proc. 46<sup>th</sup> Western Protective Relay Conference, Oct 19-22, 2020.
- [6] Donald D. Fentie, "Understanding the dynamic mho distance characteristic," in Proc. 69th Annual Conf. for Protective Relay Engineers, College Station, Texas, USA, April, 2016, pp. 1-15.
- [7] F. Calero, "Rebirth of negative-sequence quantities in protective relaying with microprocessor-based relays", in Proc. 57th Annu. Conf. Protect. Relay Eng., pp. 190-219, Apr. 2004.
- [8] G. Ziegler, "Mode of operation," in *Numerical distance protection: principles and applications*, John Wiley & Sons, 4<sup>th</sup> edn. 2011, pp. 104-105.
- [9] Schweitzer III, O. Edmund, and Jeff Roberts, "Distance relay element design," Proc. 46th Annual Conf. for Protective Relay Engineers, College Station, TX. 1993.
- [10] *MiCOM P441/P442 & P444 Numerical Distance Protection*, Schneider Electric, 2011.
- [11] *Line distance protection REL650, Version 1.3 IEC, Technical manual*, ABB, 2013.
- [12] *SIPROTEC 5, Distance and Line Differential Protection, Breaker Management for 1-Pole and 3-Pole Tripping 7SA87, 7SD87, 7SL87, 7VK87*, Siemens, 2018.
- [13] *SEL-421-4, -5, Protection, Automation and Control System, Instruction Manual*, Schweitzer Engineering Laboratories, 2017.
- [14] US Federal Energy Regulatory Commission. "Standard interconnection agreement for wind energy," Docket No. RM05-4-000 (2005).
- [15] *D60 Line Distance Relay, Instruction Manual*, GE, 2006.